Recent Results on Soft QCD Topics from ATLAS

Bormio, 55. International Winter Meeting on Nuclear Physics,

25.01.17

Andrey Minaenko, IHEP (Protvino)

on behalf of the ATLAS Collaboration

Outline

- **The ATLAS detector is designed to investigate very rare high p_T processes in the environment of high luminosities and large number (several tens) of interactions per one bunch crossing**
- **But ATLAS provides also a window onto important soft QCD processes which have large cross sections and the data for such studies are taken in special low luminosity runs**
- **These processes have intrinsic interest. They can not be predicted by a perturbative QCD. Various MC models, having a large number of adjustable tuning parameters, are used to describe them**
- **As well they are needed to understand pile-up and underlying event activity in *all* LHC measurements**
- **This presentation concerns the 4 following recent ATLAS soft QCD studies:**
  - **I. Charged-particles distributions in $\sqrt{s}$ = 13 TeV pp interactions**
    - **Phys.Lett. B (2016) 758**
  - **II. Measurement of charged-particle distributions sensitive to underlying event in $\sqrt{s}$ = 13 TeV pp collisions**
    - **arxive:1701.05390**
  - **III. Study of hard double-parton scattering in four jet events in pp collisions at $\sqrt{s}$ = 7 TeV**
    - **JHEP 11 (2016) 110**
  - **IV. Measurement of the total cross section from elastic scattering in pp collisions at $\sqrt{s}$ = 8 TeV**
    - **Phys.Lett. B (2016) 158**

I-II. Inner Detector

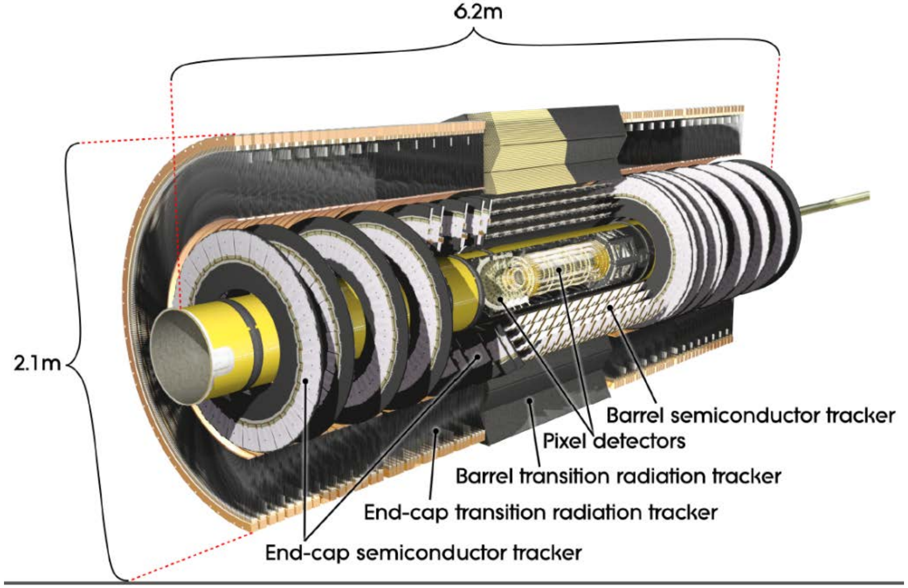

- **Studies I and II are based on the reconstructed in the Inner Detector (ID) (Figure above) charged tracks**
- **ID has full coverage in ϕ and covers the pseudorapidity range $|\eta| < 2.5$ and it is placed inside 2T axial magnetic field**
- **Its barrel (end-cap) part consists of**
  - **four (three) pixel layers**
  - **four (nine) double-layers of single-sided silicon microstrips**
  - **73 (160) layers of TRT (Transition Radiation Tracker) straws**
- **A typical track in the barrel part has 4 pixel hits, 8 SCT hits and more than 30 TRT straw hits**
- **Minimum-bias trigger scintillators (MBTS), covering region $2.07 < |\eta| < 3.86$, are used for triggering. They are mounted at each end of the ID and segmented into 12 sectors each**

I-II. Data selection, corrections

- **Special low luminosity run with <μ> = 0.005, about 9M events**
- **Trigger: one or more fired MBTS counters on either side of the ID**
- **A number of corrections used and their uncertainties included to the corresponding systematic errors**
- **The corrections account for inefficiencies due to trigger selection, vertex and track reconstruction, background from the secondary interactions**
- **The trigger efficiency is rather high (next slide) as well as a vertex reconstruction efficiency**

I-II. Trigger and Track Reconstruction Efficiency

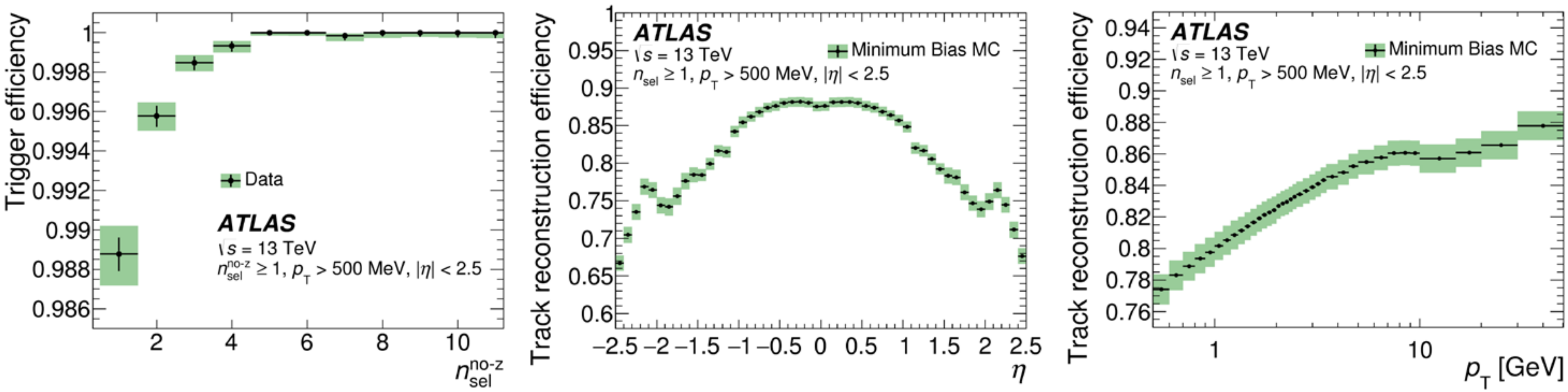

- **The primary track reconstruction efficiency, $\varepsilon_{trk}(p_T, \eta)$, is determined from the simulation**
- **ε_{trk} depends on the amount of material in the detector, due to particle interactions that lead to efficiency losses**
- **The resulting reconstruction efficiency as a function of η and p_T is shown in the above Figures together with its uncertainty**
- **The efficiency is lower at |η| > 1 due to more material in that region**
- **The total uncertainty due to imperfect knowledge of the detector material is ±0.7% in the most central region and ±1.5% in the most forward region**
- **The Bayesian unfolding is applied to the p_T and multiplicity distributions to correct from the observed track distributions to those for of primary charged particles**

I-II. Monte Carlo generators used

- **PYTHIA8:**
  - includes non-diffractive (ND) processes dominated by t-channel gluon exchange
  - and diffractive processes involving a color-singlet exchange
  - includes multi parton interactions (MPI)
  - for a hard scattering uses perturbative $2 \rightarrow 2$ QCD matrix element with leading logarithmic initial and final state parton showers
  - Lund string hadronization model
- **Herwig:**
  - for a hard scattering uses perturbative $2 \rightarrow 2$ QCD matrix element with leading logarithmic initial and final state parton showers
  - includes MPI (simpler parametrization than in PYTHIA)
  - a cluster-oriented color-disruption mechanism is used in hadronization
- **EPOS:**
  - a specialist softQCD/cosmic-ray air-shower MC generator based on an implementation of parton-based Gribov-Regge theory
  - a QCD inspired effective-field theory describing the hard and soft scattering simultaneously
- **QGSJET-II:**
  - Provides a phenomenological treatment of hadronic and nuclear interactions in the Reggeon field theory framework

I. Mean charged particle density as a function of η and p_T

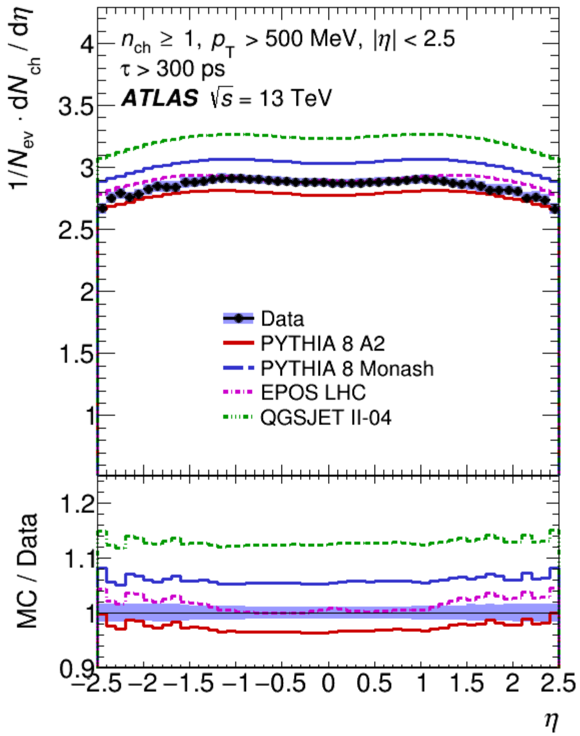

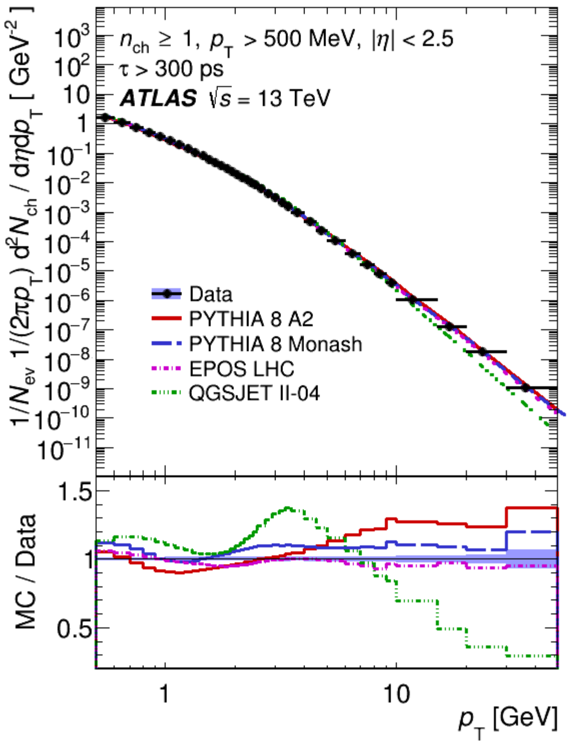

- **The mean particle density is approximately constant at 2.9 for |η| < 1 and decreases at higher |η|**
  - **EPOS describes the data well for |η| < 1 but predicts slightly larger multiplicities for larger |η|**
  - **QGSJET-II and PYTHIA8 Monash predict too large multiplicities (by 15% and 5%)**
  - **PYTHIA8 A2 – by about 3% too low in the central region but is OK in the forward region**
- **The distribution on p_T decreases by about 9 orders of value**
  - **EPOS describes the data well over the entire p_T spectrum**
  - **The PYTHIA 8 tunes describe the data well but are slightly above at large p_T**
  - **QGSJET-II gives a poor prediction over the entire spectrum**

I. The charged particle multiplicity distribution and <p_T> vs n_{ch}

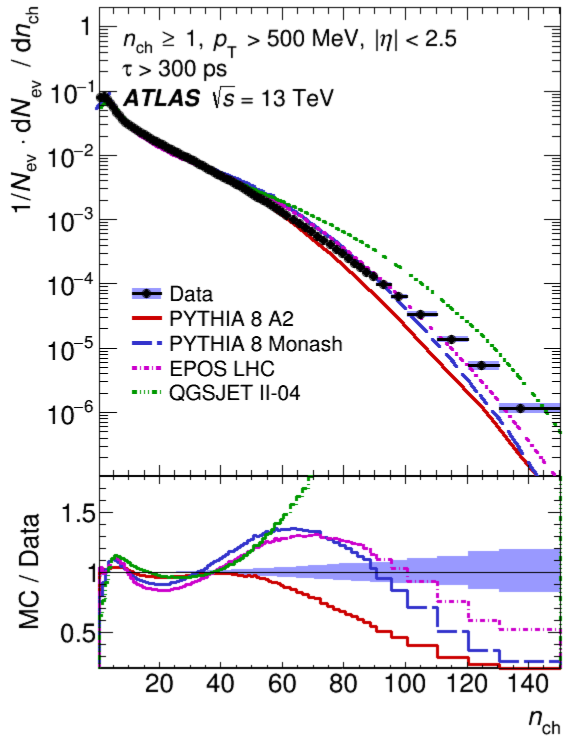

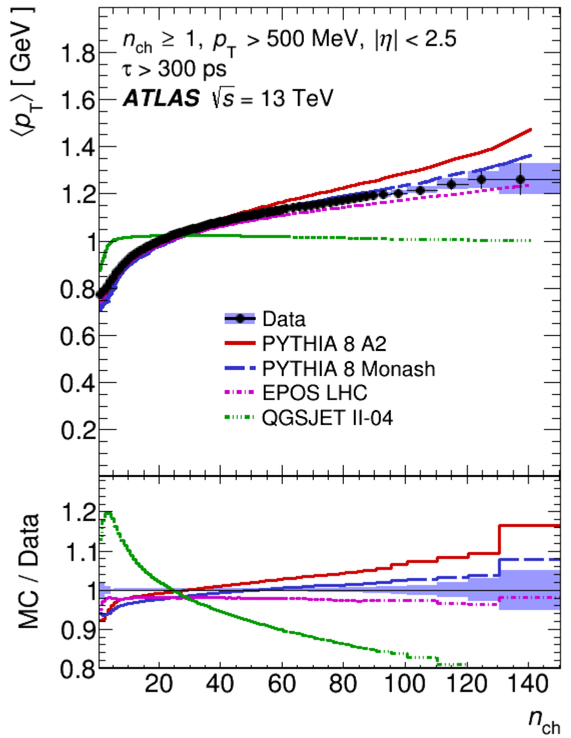

- **The charged particle multiplicity distribution decreases by 5 orders. The high n_{ch} region has significant contribution from events with numerous MPI**
  - **All the models describes the data satisfactory in the region n_{ch} < 30-50 but fail at higher n_{ch}**
  - **At high n_{ch} the strongest deviations are for QGSJET-II and PYTHIA8 A2**
- **<p_T> rises with n_{ch} from 0.8 to 1.2 GeV. The increase is modelled by a color reconnection mechanism in PYTHIA8 or by the hydrodynamical evolution model used in EPOS**
  - **EPOS predicts slightly lower <p_T>, but describes the dependence on n_{ch} well**
  - **The PYTHIA8 tunes predict a steeper rise of <p_T> with n_{ch} than the data**
  - **QGSJET-II predicts <p_T> of ~ 1 GeV, with very little dependence on n_{ch}**

I. Energy dependence of the charged particles density at η = 0

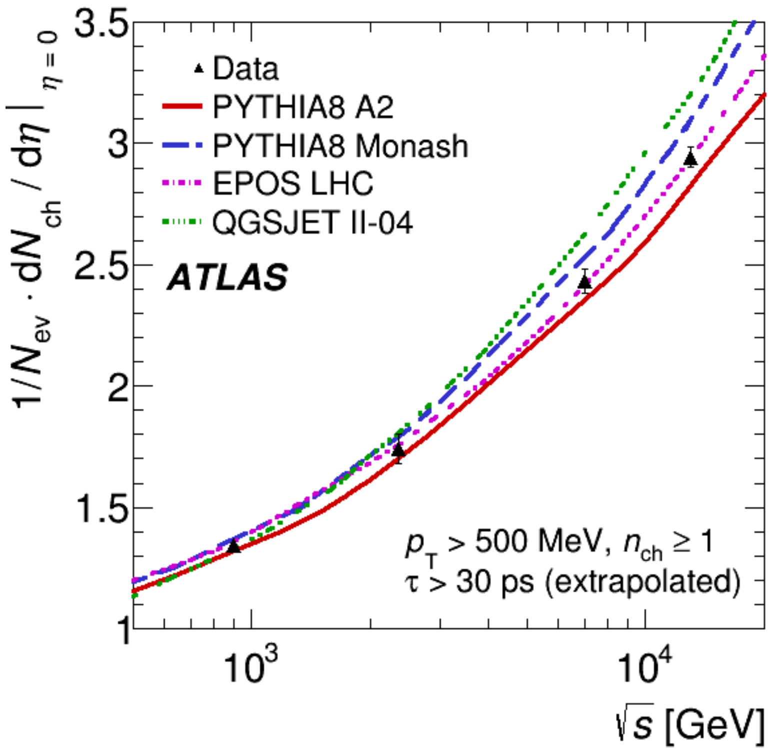

- **The mean number of primary charged particles in the central region is 2.874 ± 0.001 (stat.) ± 0.033 (syst.)**
- **The value increases by a factor of 2.2 when $\sqrt{s}$ increases by a factor of about 14 from 0.9 TeV to 13 TeV**
- **EPOS and PYTHIA8 A2 describe the dependence very well**
- **PYTHIA8 Monash and QGSJET-II predict a steeper rise in multiplicity with c.m.s. energy**

Conclusions

- **Primary-charged-particle multiplicity measurements with the ATLAS detector using pp interactions at $\sqrt{s}$ = 13 TeV are presented**
- **The results highlight clear difference between MC models and the measured distributions**
- **EPOS reproduces data the best, PYTHIA8 A2 and Monash give reasonable descriptions of the data and QGSJET-II provides the worst description**

II. Underlying event with leading p_T charged particle

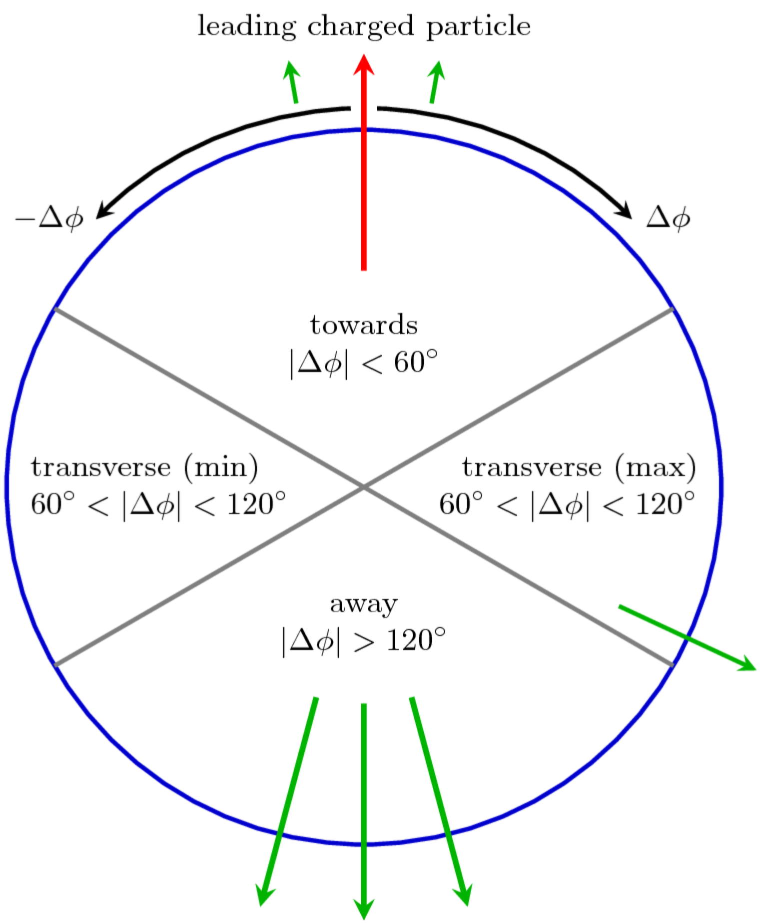

- **Underlying event is defined as activity accompanying any hard scattering in a event**
- **It includes**
  - **Partons not participating in a hard scattering (beam remnants)**
  - **Multiple parton interactions**
  - **Initial state gluon radiation (ISR)**
- **It is impossible to separate the UE from the hard scattering process on an event by event base**
- **However distributions have been measured which are sensitive to the properties of the UE**
- **These are the distributions of particles in the transverse regions (Figure)**
- **The figure illustrates distribution of charged particles in the transverse to the beam plane with respect to the leading p_T charged particle**
- **The towards and away regions contain products of the hard scatter mostly**

II. Trans-min region

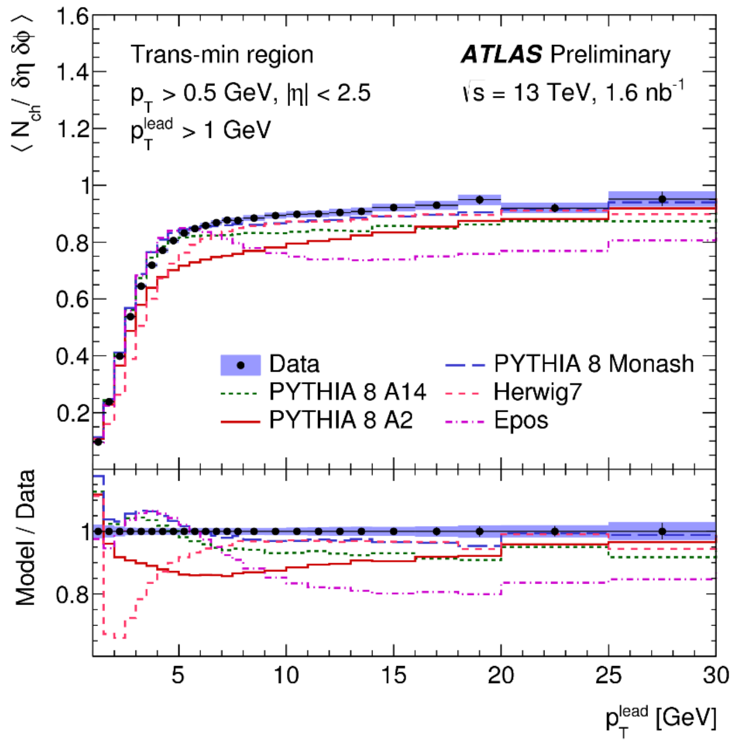

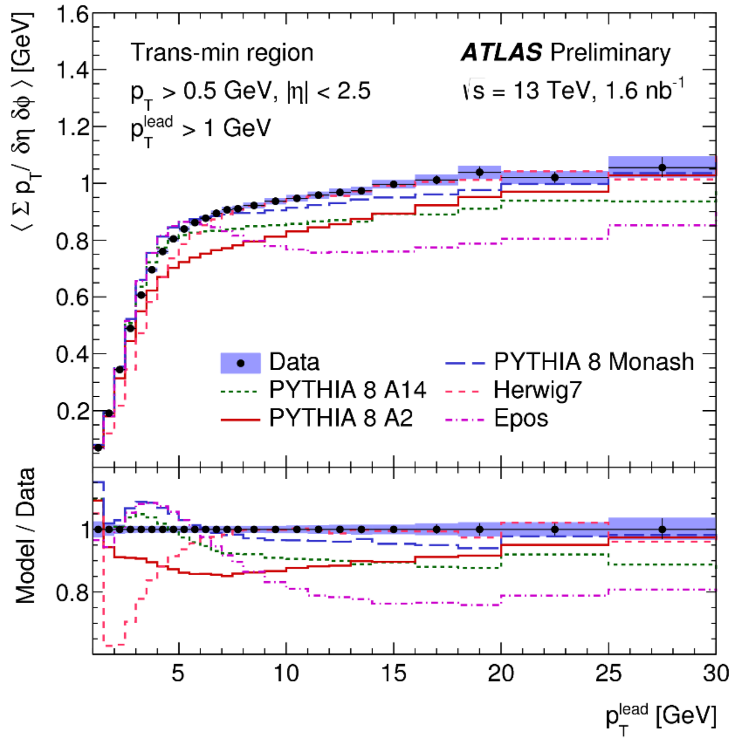

- **Trans-min region most sensitive to MPI and hard process contamination is small: the distributions are rather flat above p_T = 5 GeV**
- **EPOS and PYTHIA8 A2 are too low at the plateau region**
- **Herwig7 gives one of the best descriptions at the plateau but severe undershoots transition region below p_T = 5 GeV**

II. Trans-max region

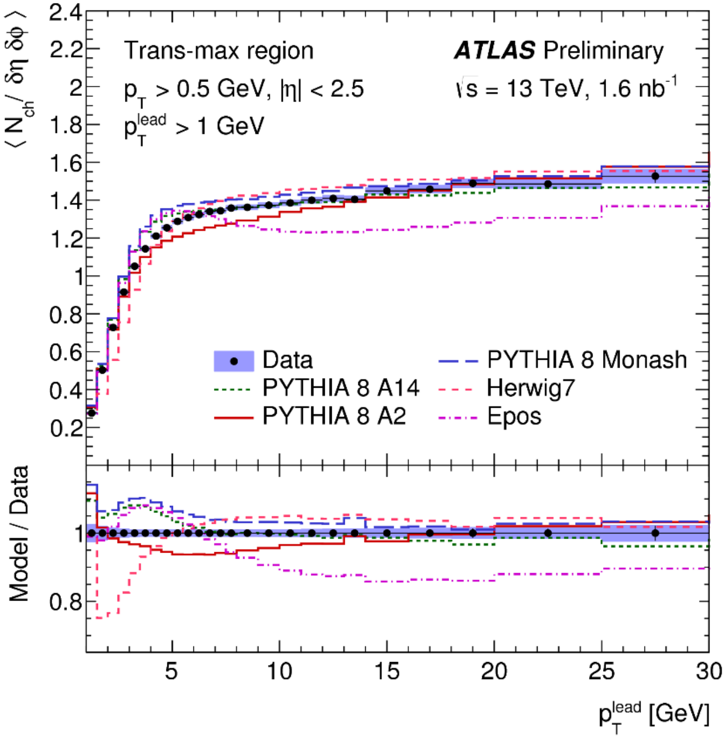

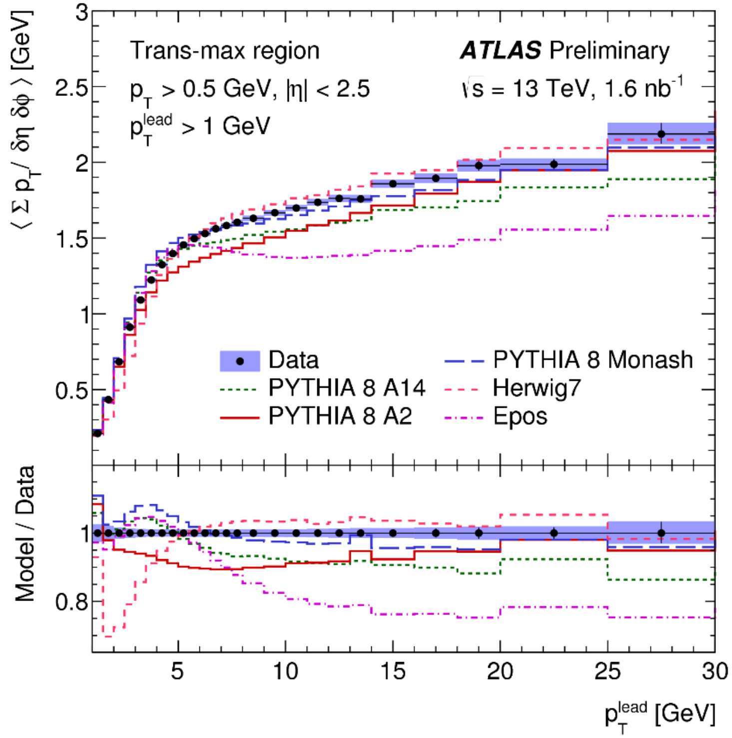

- **The trans-max region has larger hard process contamination: the rise in the plateau region is stronger and its mean level is noticeably larger**
- **In general MC generators describes the data better than for the trans-min**
- **EPOS strongly undershoots data at $p_T > 10$ GeV**
- **Herwig7 again undershoots $p_T < 5$ GeV**

II. Conclusions

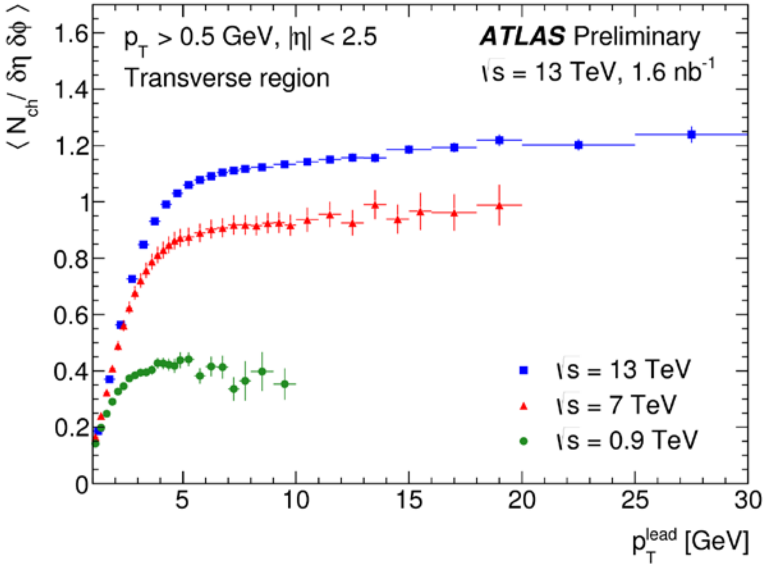

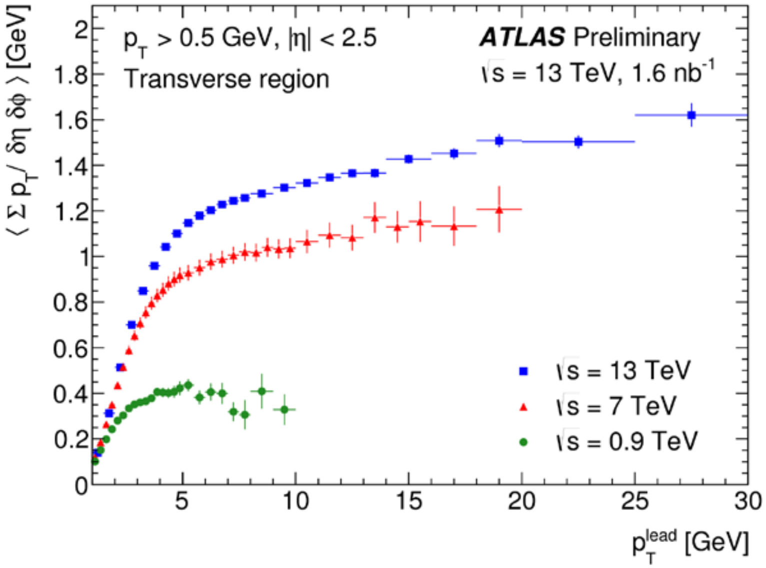

- **A number of distributions sensitive to properties of the UE are presented**
- **Present measurement completes previous ATLAS measurements at lower energies (above figures)**
- **An increase of UE activity of approximately 20% is observed when going from 7 TeV to 13 TeV pp collisions**
- **Comparison against prediction from several MC generator tunes indicate that for most observables the models describe UE data to better than 5% accuracy**
- **EPOS gives the worst predictions**
- **The data can be used to improve MC tunes**

III. Hard double parton scattering in 4-jet events

$$\hat{\sigma}^{\mathrm{DPS}}_{(\mathrm{A,B})} = \frac{1}{1+\delta_{\mathrm{AB}}} \frac{\hat{\sigma}_{\mathrm{A}} \hat{\sigma}_{\mathrm{B}}}{\sigma_{\mathrm{eff}}},$$

$$\Longrightarrow \quad \sigma_{\mathrm{eff}} = \frac{1}{1+\delta_{\mathrm{AB}}} \frac{\hat{\sigma}_{\mathrm{A}} \hat{\sigma}_{\mathrm{B}}}{f_{\mathrm{DPS}} \cdot \hat{\sigma}^{\mathrm{tot}}_{(\mathrm{A,B})}}$$

Kroneker δ =1, if A and B the same

fraction of DPS events

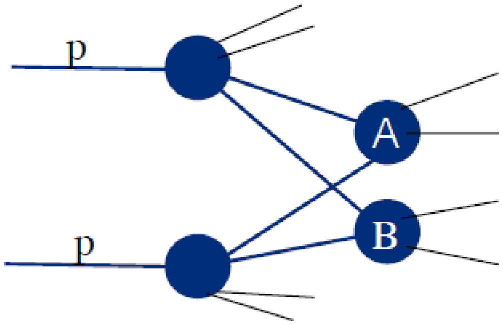

$$\sigma_{\mathrm{eff}} = \frac{1}{1+\delta_{\mathrm{AB}}} \frac{1}{f_{\mathrm{DPS}}} \frac{\sigma^{\mathrm{A}}_{2j} \sigma^{\mathrm{B}}_{2j}}{\sigma_{4j}}$$

- **σ_{eff} is an effective cross section (to be found)**
  - **phenomenological parameter describing the effective overlap between the interacting hadrons**
  - **determines the overall size of DPS cross section**
  - **Assumed to be process and cut independent**
- **Data taken in pp collisions at $\sqrt{s}$ = 7 TeV during 2010, <μ> = 0.41, integrated luminosity 37.3 pb^{-1}**

III. Event selection, templates

- **Single vertex events only**
- **Use anti-k_T jets with R = 0.6 found in calorimeters at $|\eta| < 4.4$**
- **4-jet event selection: $N_{jet} \geq 4$, $p_T^1 > 42.5$ GeV, $p_T^{2,3,4} > 20$ GeV**
- **Di-jet samples $N_{jet} \geq 2$, A: $p_T^{1,2} > 20$ GeV; B: $p_T^1 > 42.5$ GeV, $p_T^2 > 20$ GeV**
- **4-jet and B samples are subsamples of sample A**
- **AHJ MC: Alpgen (2 → n, n up to 5) + Jimmi (MPI) + Herwig (hadronization)**
- **Event record of AHJ is used to distinguish between (2 → 4) and (two 2 → 2) processes**
- **Sample SPS: all 4 jets from one hard scatter, based on AHJ MC**
- **Sample complete DPS (cDPS): 2 jets from 1st hard scatter, 2 jets from 2nd one. Obtained by overlaying two di-jet data events**
- **Sample semi DPS (sDPS): 3 jets from 1st hard scatter, 1 jet from 2nd one. Obtained by overlaying two di-jet data events**
- **Template fit is used to determine $f_{DPS} = f_{cDPS} + f_{sDPS}$**

III. Discriminating variables

- **21 discriminating variables are used to classify events as belonging to SPS (ξ_{SPS}), cDPS (ξ_{cDPS}), or sDPS (ξ_{sDPS}): $\xi_{SPS} + \xi_{cDPS} + \xi_{sDPS} = 1$**
- **Neural network is used for event classification**

$$\Delta_{ij}^{p_T} = \frac{\left|\vec{p}_T^{\,i} + \vec{p}_T^{\,j}\right|}{p_T^i + p_T^j}; \quad \Delta\phi_{ij} = \left|\phi_i - \phi_j\right|; \quad \Delta y_{ij} = \left|y_i - y_j\right|;$$

$$|\phi_{1+2} - \phi_{3+4}|; \qquad |\phi_{1+3} - \phi_{2+4}|; \qquad |\phi_{1+4} - \phi_{2+3}|;$$

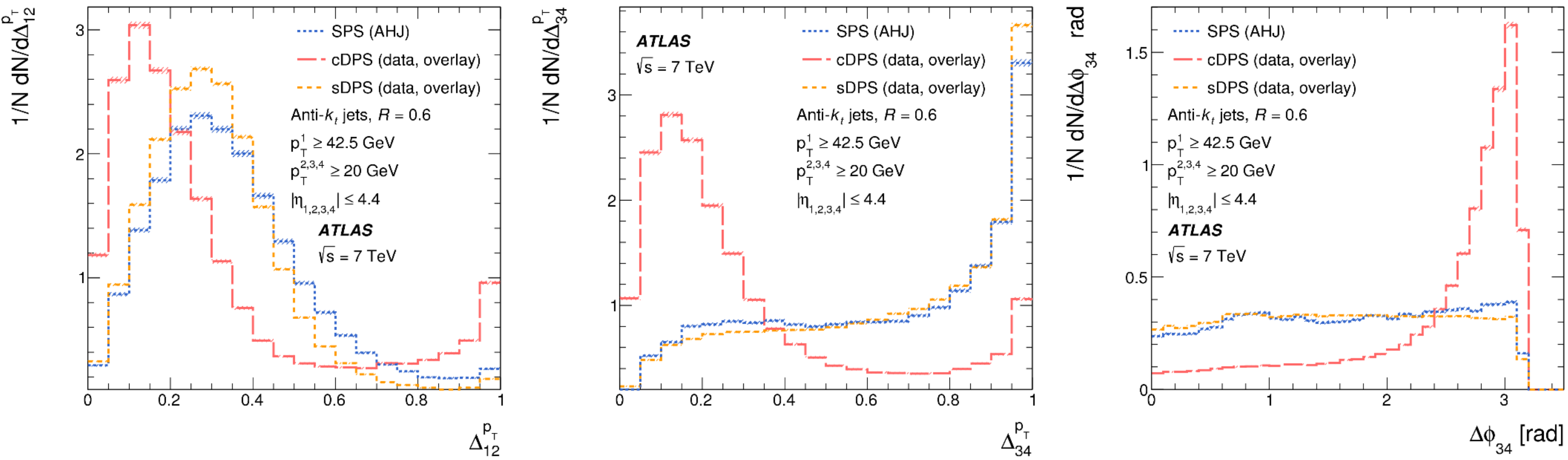

III. NN output for test samples

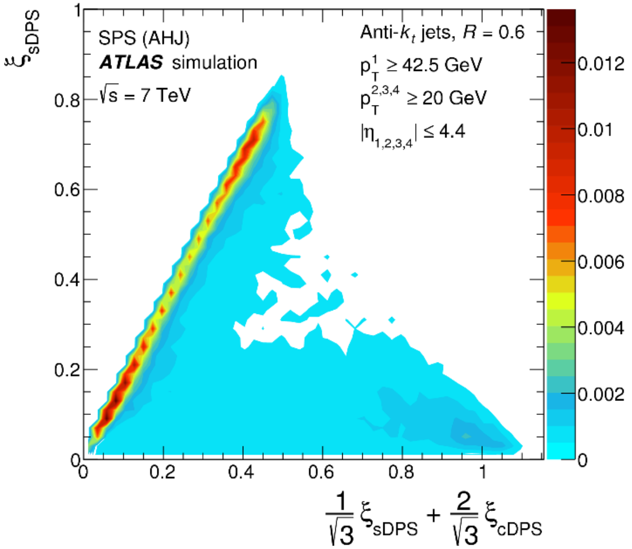

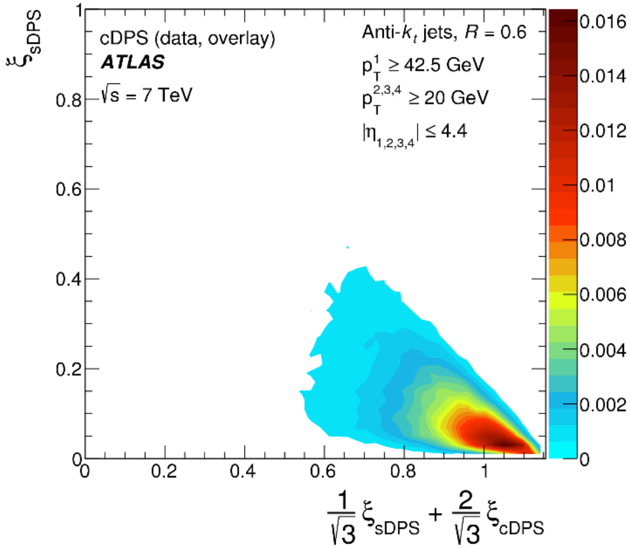

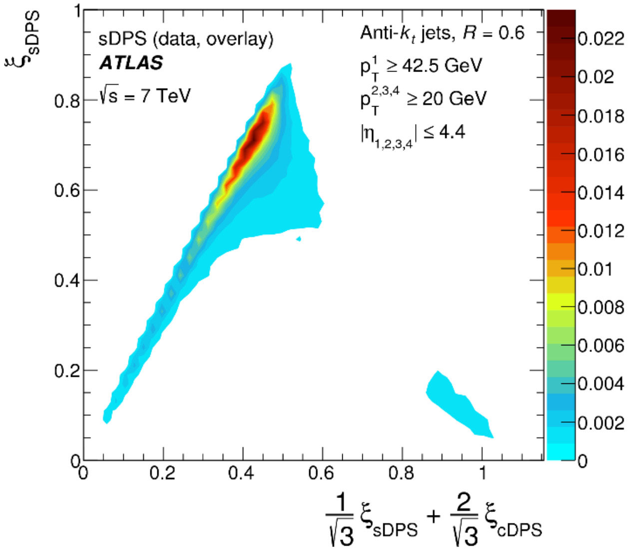

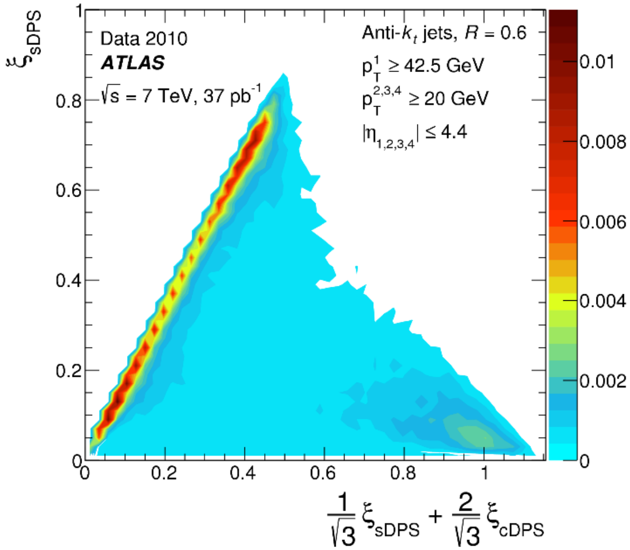

III. Results

- χ^2 minimization with Minuit to find f_{cDPS} and f_{sDPS}
- $D = (1 - f_{cDPS} - f_{sDPS})*M_{SPS} + f_{cDPS}*M_{cDPS} + f_{sDPS}*M_{sDPS}$
- Here **D** is ternary data distribution
- M_{SPS}, M_{cDPS} and M_{sDPS} are ternary distributions in test samples normalized to measured 4-jet cross section
- Different sources of systematic uncertainties were taken in to account and propagated to the final results
- The dominating source is jet energy scale (JES) uncertainty: about 4.5% in the central region and rising to about 10% in the forward one. It gives about 30% uncertainty in the final results

$$f_{DPS} = 0.092\ ^{+0.005}_{-0.011}\ (\text{stat.})\ ^{+0.033}_{-0.037}\ (\text{syst.}),$$

$$\sigma_{\text{eff}} = 14.9\ ^{+1.2}_{-1.0}\ (\text{stat.})\ ^{+5.1}_{-3.8}\ (\text{syst.})\ \text{mb}$$

III. Results overview

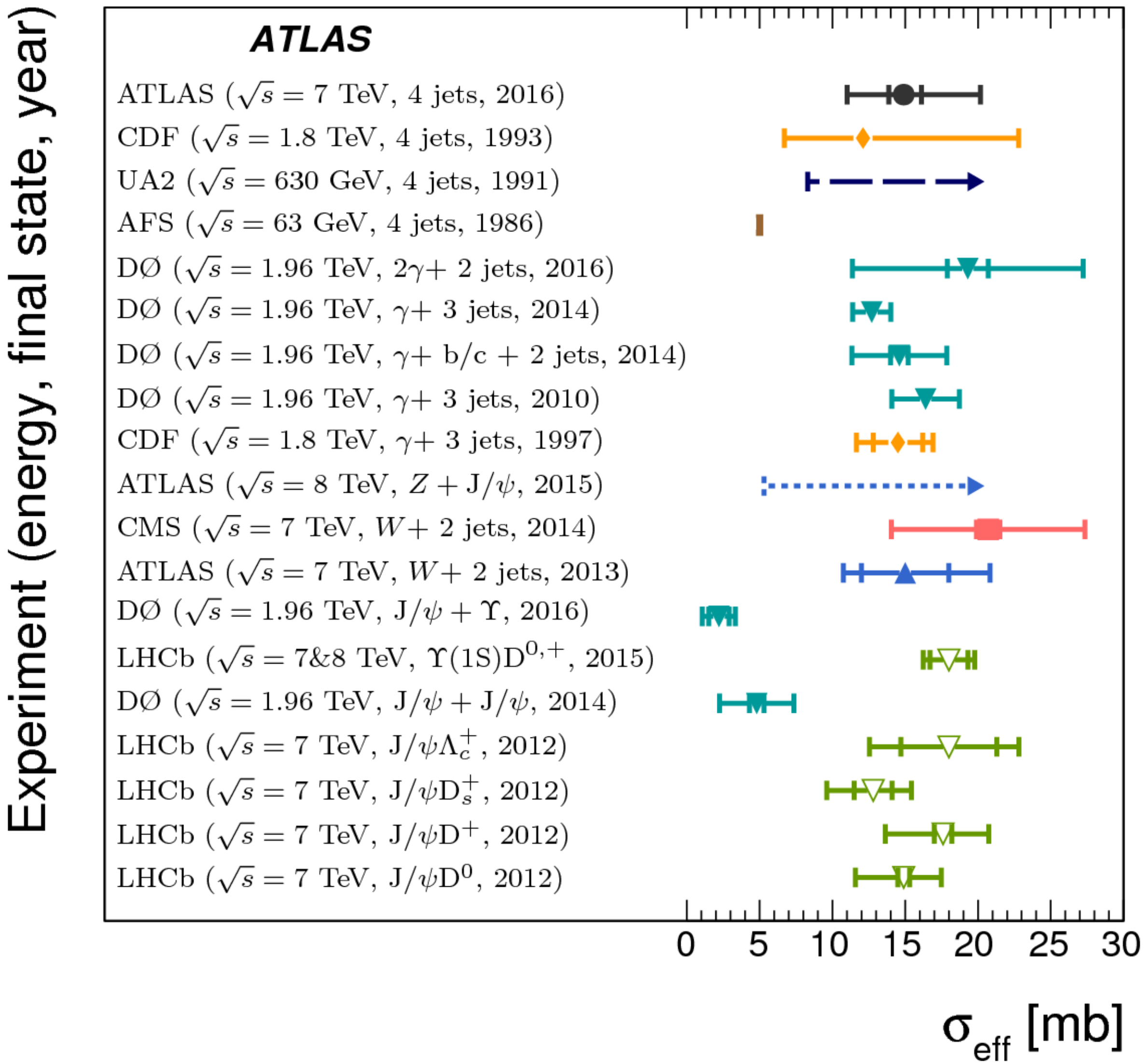

IV. Total and elastic cross sections

- **Optical theorem relates total pp cross section to the elastic-scattering amplitude extrapolated to the forward direction**

$$\sigma_{tot} = 4\pi * \mathrm{Im}(f_{el})_{t\to 0}$$

- **ATLAS uses optical theorem and luminosity-dependent method of the total cross section extraction. With this method**

$$\sigma_{tot}^2 = \frac{16\pi(hc)^2}{1+\rho^2}\frac{d\sigma_{el}}{dt}\Big|_{t\to 0}$$

- **Where ρ = 0.1362 represents a small correction arising from the ratio of the real to the imaginary part of the elastic-scattering amplitude**

IV. ALFA detector, data taking

- **ALFA detector is used to record elastic-scattering data**
- **Consists of Roman Pot (RP) tracking detector stations placed at 237 m (inner) and 241 m (outer) on either side of the ATLAS IP**
- **Each station houses two scintillating fibre detectors with a spatial resolution of about 35 μm**
- **The detectors are supplemented with trigger counters consisting of plain scintillator tiles**
- **The data recorded in a single low luminosity run with special high β^* optics for pp interactions at $\sqrt{s}$ = 8 TeV**
- **3.8 M selected elastic events**
- **Measure elastic track positions at ALFA to get the scattering angle Θ and thereby the t-spectrum dσ/dt**
- **To calculate Θ from the measured tracks the transport matrix elements of the beam optics are used**

IV. ALFA detector

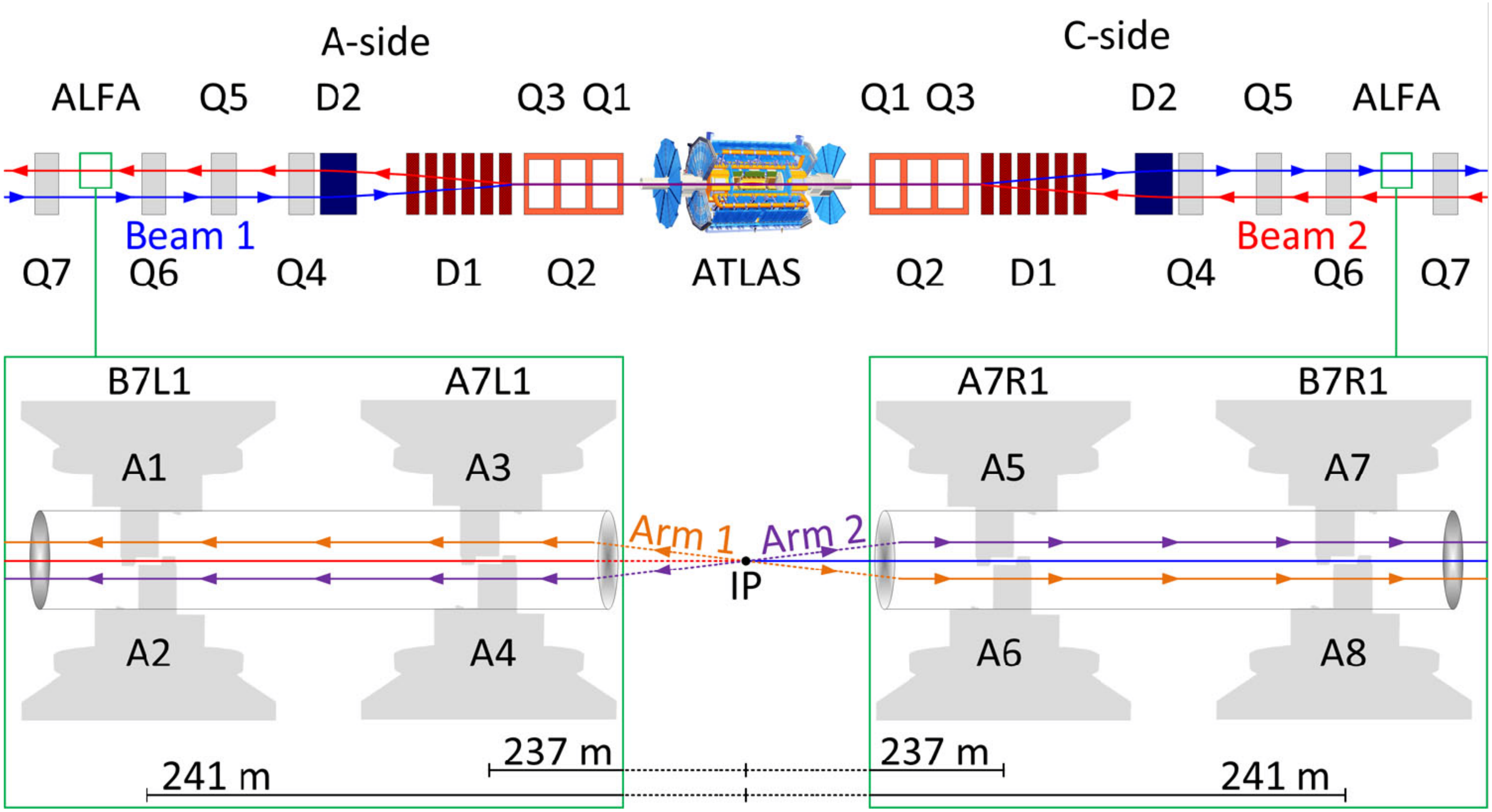

IV. Analysis of elastic data

- **Data-driven method to calculate the reconstruction efficiency of about 90%**
- **Tuning of the beam optics model with ALFA constrains → effective optics**
- **Trigger efficiency is very high ~99.9%; determined from data stream with looser conditions**
- **Dedicated luminosity determination resulting in a small uncertainty of 1.5%**

$$\left(\frac{d\sigma}{dt}\right)_i = \frac{1}{t_i} \cdot \frac{\mathrm{M}^{-1}\left[N_i - B_i\right]}{A_i \cdot \varepsilon^{reco} \cdot \varepsilon^{trig} \cdot \varepsilon^{DAQ} \cdot \mathrm{L}_{\mathrm{int}}}$$

- **Δt_i : the width of the bins in t**
- **A : acceptance(t)**
- **M^{-1}: symbolizes the unfolding procedure applied to the background subtracted number of events $N_i - B_i$**
- **ε^{reco}: event reconstruction efficiency**
- **ε^{trig}: trigger efficiency**
- **ε^{DAQ}: the dead time correction**
- **L_{int}: the integrated luminosity**

IV. Fitting formula for dσ/dt

- **The theoretical prediction used to fit the elastic data consists of the Coulomb term, the Coulomb-Nuclear-Interference term and the dominant Nuclear term**

$$\frac{d\sigma}{dt} = \frac{4\pi\alpha^2(\hbar c)^2}{|t|^2} \cdot G^4(t)$$ Coulomb

CNI $$- \sigma_{\text{tot}} \cdot \frac{\alpha G^2(t)}{|t|} \left[\sin(\alpha\phi(t)) + \rho\cos(\alpha\phi(t))\right] \cdot \exp\frac{-B|t|}{2}$$

Nuc. $$+ \sigma_{\text{tot}}^2 \frac{1+\rho^2}{16\pi(\hbar c)^2} \cdot \exp(-B|t|) \;.$$

ρ	0.1362
Λ	0.71 GeV^2
ϕ_C	0.577

$$G(t) = \left(\frac{\Lambda}{\Lambda+|t|}\right)^2 \;,$$ Proton dipole form factor

$$\phi(t) = -\ln\frac{B|t|}{2} - \phi_C \;,$$ Coulomb phase

Fit results

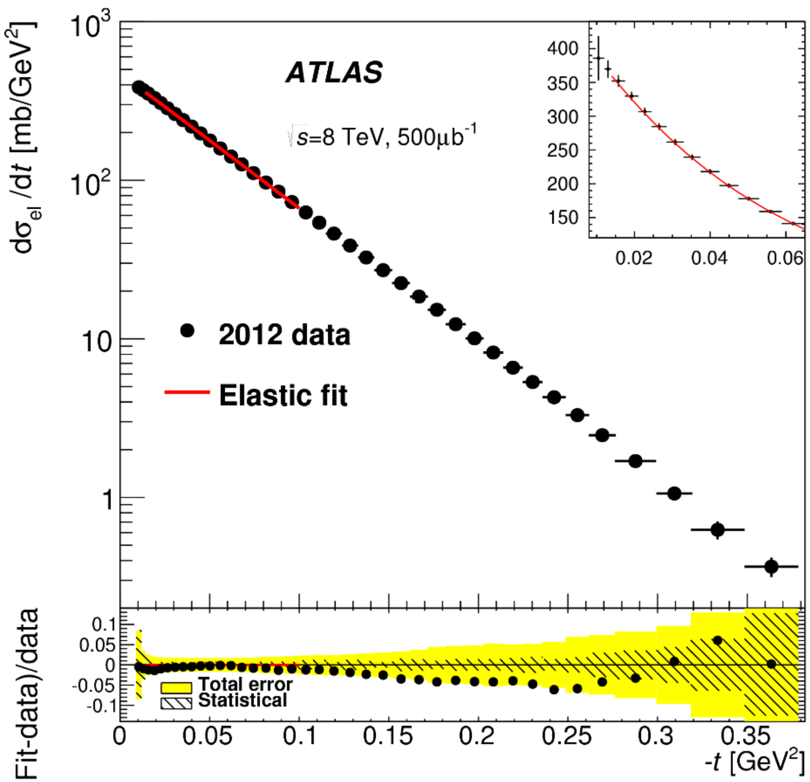

(b)

- The fit includes experimental systematic uncertainties in the χ^2
- Main systematics
  - t-independent: luminosity ±1.5%
  - t-dependent: beam energy ±0.65%
- The fit range is set to –t[0.014, 0.1] GeV^2, where possible deviations from exponential form of the nuclear amplitude are expected to be small
- The extrapolation uncertainty is evaluated by a variation of the fit range

- **σ_{tot} = 96.07 ± 0.18(stat.) ± 0.85(exp.) ± 0.31(extr.)**
- **B = 19.74 ± 0.05(stat.) ± 0.16(exp.) ± 0.15(extr.)**

IV. Energy evolution

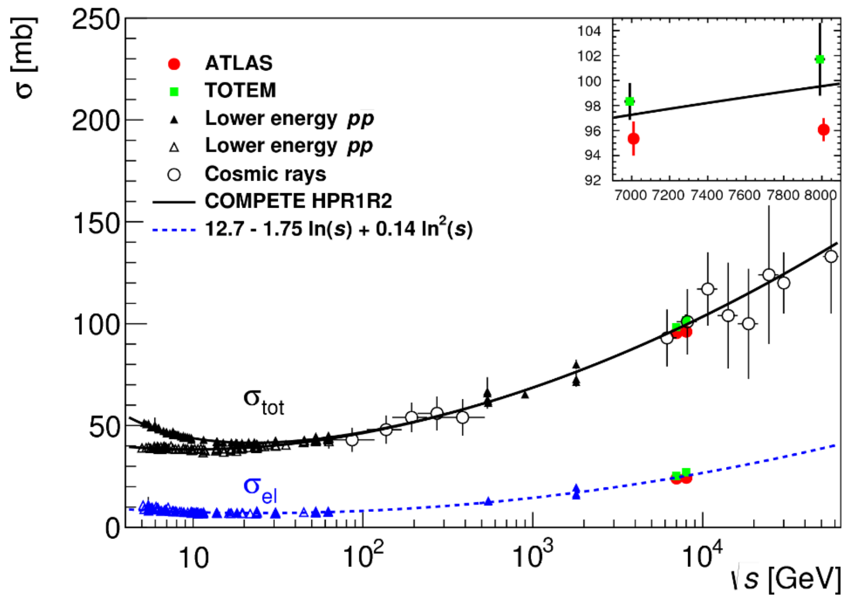

(a)

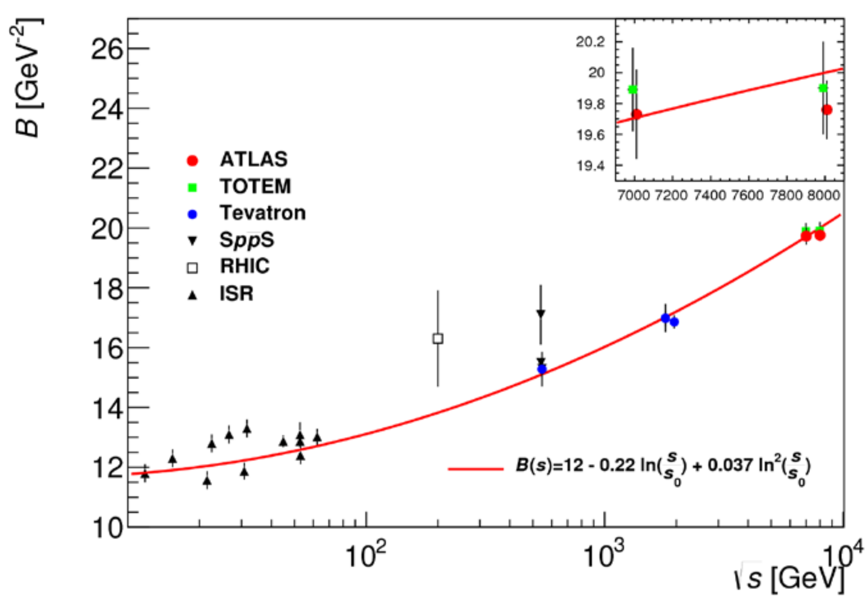

(b)

- **Comparison with COMPETE model Chin.Phys. C, 38, 090001 (2014) for the evolution of the total cross section. High accuracy of the ATLAS data due to precise luminosity measurement**

- **Comparison with a model from Schegelsky and Ryskin Phys.Rev. D85, 094024 (2012) for the evolution of the nuclear slop**

Summary

- **Primary-charged-particle multiplicity measurements with the ATLAS detector using pp interactions at $\sqrt{s}$ = 13 TeV were done**
- **The results highlight clear difference between MC models and the measured distributions**
- **EPOS reproduces data the best, PYTHIA8 A2 and Monash give reasonable descriptions of the data and QGSJET-II provides the worst description**
- **A number of distributions sensitive to properties of the UE are presented for pp interactions at $\sqrt{s}$ = 13 TeV**
- **EPOS fails to describe the data properly contrary to the minimum bias event description, for which EPOS is the best**
- **Comparison against prediction from several other MC generator tunes indicate that for most observables the models describe UE data to better than 5% accuracy**
- **Hard double parton scattering in 4-jet events is investigated in pp interactions at $\sqrt{s}$ = 7 TeV**
- **The phenomenological DPI parameter σ_{eff} is extracted**
- **Distribution dσ/dt for proton-proton elastic scattering at $\sqrt{s}$ = 8 TeV is measured and used to estimate σ_{tot} = 96.07 ± 0.18(stat.) ± 0.85(exp.) ± 0.31(extr.)**